Tailoring the Shape of Metal Ad-Particles by Doping the Oxide Support**

Xiang Shao, Stefano Prada, Livia Giordano, Gianfranco Pacchioni, Niklas Nilius,* and Hans-Joachim Freund*

Doping is a versatile yet little examined approach to tailor the physical and chemical properties of oxide thin films. By means of scanning tunneling microscopy (STM), we demonstrate how tiny amounts of Mo embedded in a CaO matrix change the growth behavior of gold. Whereas 3D deposits are formed on the pristine oxide surface, strictly 2D growth prevails on the doped material. The crossover in particle shape is driven by charge-transfer processes from the Mo dopants into the Au islands, as elucidated with density-functional theory (DFT) calculations.

Optimizing the structural and electronic properties of supported metal catalysts to augment their conversion and selectivity is a goal of catalysis research. Various key parameters that govern the catalytic performance have been identified to date, for example, selecting proper material combinations and maximizing the dispersion of the active species. Special emphasis was placed on controlling the properties of the metal centers on the catalyst surface, that is, their size, shape, crystallinity, and charge state. In gold catalysis, for example, small raft-like deposits with amorphous structure and non-zero charge state were found to be more active than their bulk-like and neutral counterparts.[1–4]

There are different approaches to manipulate the properties of metal deposits. Whereas their size and density can be tuned by introducing anchoring sites into the oxide surface, for example, defects[4] or hydroxyl groups,[5] their charge state is controlled by adjusting the metal–support interactions.[6] Oxygen vacancies or structural electron traps, for example, were found to initiate a charge transfer into the ad-metal. On ultrathin oxide films, even spontaneous charging takes place as electrons tunnel from the substrate into the metal deposits.[7,8] Oxide doping might open new, versatile routes to tune particle–support interactions.[9–11] Whereas "overvalent" dopants produce excess electrons in the host oxide that can be transferred into suitable adsorbates, "undervalent" impurities promote the formation of holes in the oxide electronic structure that might be filled with electrons from the metal deposits. Such a charge transfer has direct consequences on the equilibrium shape of the ad-particles, as it enhances the metal oxide adhesion as well as the Coulomb forces within the confined metallic systems.[8,12,13] The presence of dopants also alters the formation energy of oxide defects that may act as nucleation centers and hence stabilize the dispersion of the active species.[14] Although a good theoretical understanding could be achieved on doping effects in supported metal catalysts, experimental studies performed at a fundamental level are still scarce.

Herein, we investigate the influence of Mo dopants on the growth of Au particles on CaO(001) films, by STM and DFT. The doping is realized by adding 2 atm % of Mo to the Ca/O vapor that is used for growing oxide films of 60 monolayer (ML) thickness.[15] The topmost layers are always prepared without dopants to suppress Mo segregation to the surface. The presence of Mo in the CaO matrix is confirmed with Auger spectroscopy (Figure 1 a). Whereas only the Ca and O Auger transitions at 250, 290 ,and 512 eV are detected in the pristine oxide, Mo-specific peaks (around 200 eV) appear in doped films with a sufficiently thin capping layer. STM images of molybdenum-doped CaO films (CaO_{Mo}) display atomically flat and defect poor surfaces, covered with oxide terraces of 20 nm diameter, independent of the doping level (Figure 1 b). The predominant defects are dislocation lines that originate from the coalescence of neighboring oxide islands and are involved in compensating the substrate-induced lattice strain.[15] For doped films with more than ten capping layers, no additional defects are revealed on the surface. Apparently,

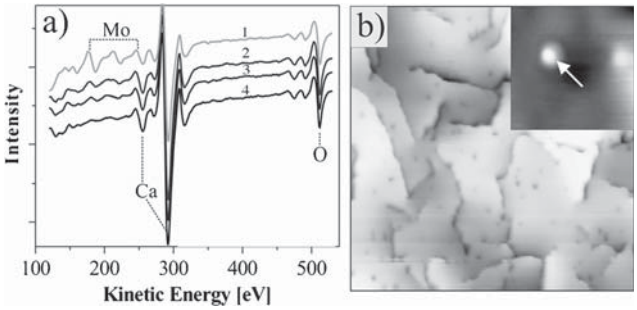

Figure 1. a) Auger spectra of pristine and Mo-doped CaO films covered with a thin Mo-free capping layer. The top curve has been taken after Mo deposition directly onto the surface. 1) 60 ML CaO + 2 ML Mo; 2) 50 ML CaO_{Mo} + 10 ML cap; 3) 40 ML CaO_{Mo} + 20 ML cap; 4) 60 ML CaO. b) STM image of a doped CaO film (100×100 nm^2). Inset: single Mo impurity, as observed in a film without capping layer (5×5 nm^2).

[*] Dr. X. Shao, Dr. N. Nilius, Prof. H.-J. Freund
Fritz-Haber-Institut der Max-Planck-Gesellschaft
Faradayweg 4–6, 14195 Berlin (Germany)
E-mail: nilius@fhi-berlin.mpg.de

S. Prada, Dr. L. Giordano, Dr. G. Pacchioni
Dipartimento di Scienza dei Materiali, Università di Milano-Bicocca
via Cozzi 53, 20125 Milano (Italy)
E-mail: livia.giordano@mater.unimib.it

[**] We are grateful for financial support from the DFG within the Cluster of Excellence 'Unicat' and thank the Regione Lombardia (LISA) and CILEA for a CPU grant.

the caps are sufficiently thick to inhibit Mo segregation even during high-temperature treatments (up to 1000 K). When using thinner caps, atom-sized protrusions can be detected in the STM, which are assigned to individual Mo species (Figure 1 b, inset).

Deposition of 0.7 ML Au at 300 K leads to the formation of metal particles. On pristine films, the deposits preferentially nucleate along the CaO dislocation lines and adopt pronounced 3D shapes (Figure 2 a) with a height to diameter ratio of 0.35 ± 0.10. The observed Volmer–Weber growth is

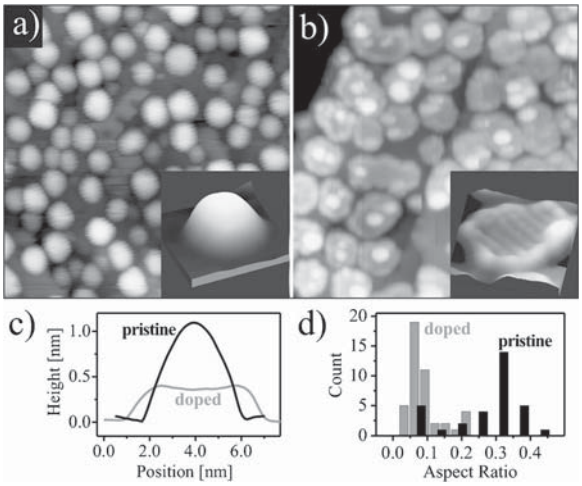

Figure 2. STM images of 0.7 ML Au on a) pristine and b) doped CaO films (50×50 nm^2). The insets display close-ups of two characteristic particles (10×10 nm^2) with the corresponding height profiles plotted in (c). d) Histogram of particle aspect ratios on doped and pristine films.

characteristic for metals on wide-band-gap materials and reflects the small adhesion between ad-layer and inert oxide support.[16] In contrast, on the doped films, randomly distributed Au islands of monolayer height and aspect ratios of 0.07 ± 0.02 develop (Figure 2 b). These islands have hexagonal shapes, indicating growth along Au[111], and display a characteristic stripe pattern on their surface that is assigned to a Moiré structure formed between the square CaO and the hexagonal Au(111) lattice. The patterns occur with different orientations, indicating a rather loose Au-CaO interfacial registry. However, the mere appearance of monolayer islands suggests that the Mo impurities have a considerable impact on the Au–CaO adhesion.

To shed light on the role of the dopants, we have performed DFT calculations on a five-layer CaO(001) slab with one Mo ion substituting a Ca^{2+} species (2 % Mo content). The calculations were carried out at the PBE level, but have been confirmed with test runs using hybrid HSE functionals. Without dopants, the Au adsorbs with 1.35 eV on top of a surface oxygen ion (Figure 3). The binding strength nearly triples in presence of a Mo species, even if the dopant is located well below the surface. Clearly, the Au–Mo interaction is preserved over large distances and independent of direct orbital overlap. Furthermore, the preference for binding to a surface oxygen atom is lost and cationic, anionic, and hollow sites become equally preferred sites for Au adsorption on the doped CaO films. For charge-neutrality reasons, the substituting Mo should adopt the $2+$ charge state of a rocksalt cation, which implies the Mo center must donate its 5s electrons to the neighboring ions, but retains the four electrons in the Mo 4d shell. This scenario is confirmed with HSE calculations for a single Mo in a bulk CaO environment, which find the low-spin $(t_{2g})^4(e_g)^0$ configuration as ground state and the high-spin $(t_{2g})^3(e_g)^1$ state at 0.5 eV higher energy.[17] Also with PBE, the $(t_{2g})^4(e_g)^0$ configuration remains energetically favorable however the e_g levels move into the CaO conduction band due to an under-estimation of the band gap with this functional (Figure 4 a). STM conductance spectra taken on 8 ML thick doped films confirm the existence of localized states in the gap region. Their assignment to specific Mo 4d-levels is hampered by the proximity of the metal substrate that is neglected in the calculations (Figure 4 b). However, no conductance data could be acquired on thicker films because of the vanishing tunneling probability of electrons through the CaO gap region.

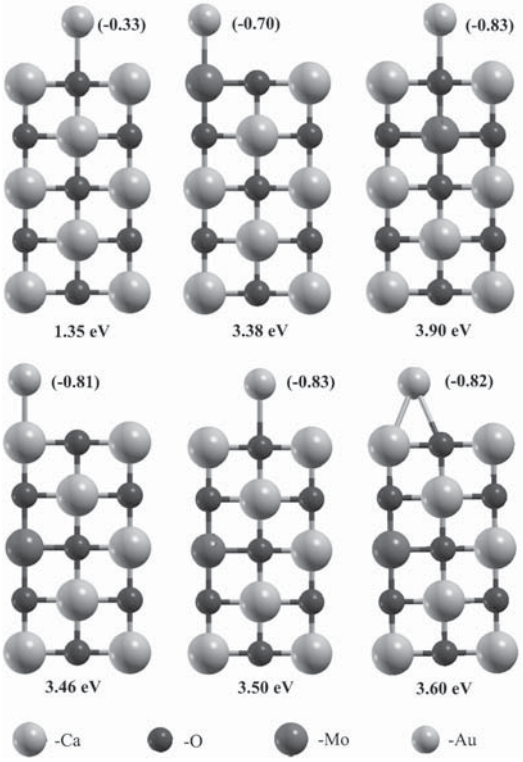

Figure 3. PBE binding energies and Bader charges (in parenthesis) for Au adsorbed on CaO(001) with a Mo impurity in various positions.

The PBE calculations suggest the Mo^{2+} charge state to be instable against electron transfer, either into CaO defect states,[18,19] or into ad-species with acceptor character. Whereas electron trapping in the oxide film could not be confirmed, a charge transfer into the Au deposits is fully compatible with both the theoretical and experimental results. On pristine CaO, the Au atoms are neutral, as deduced from their half-filled 6s level, and bind to the surface

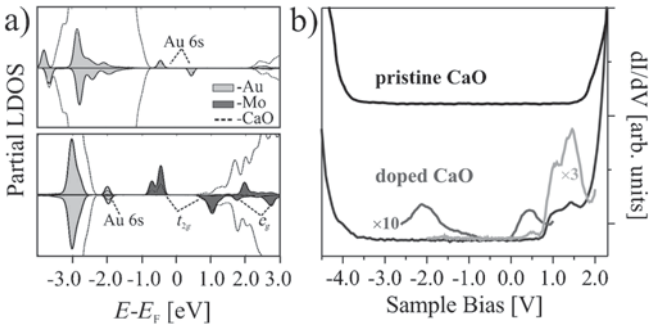

Figure 4. a) PBE projected density-of-states (DOS) calculated for non-doped (top) and doped (bottom) CaO films in presence of an Au ad-atom. b) STM conductance spectra taken on pristine and doped films of 8 ML thickness without gold. Several CaO gap states are discernable in the doped case.

mainly through O 2p–Au 5d hybridization (Figure 4 a). Upon doping, the Au 6s orbital shifts below the Fermi level and becomes doubly occupied, through a charge transfer from the Mo 4d state. This leads to an increased Bader charge and a vanishing magnetization of the bound gold atoms (Figures 3 and 4 a). Concomitantly, the oxidation of the Mo dopant is detected, as the occupancy of the Mo 4d levels changes to $(t_{2g})^3(e_g)^0$ and the Mo charge state rises to $3+$. The electron transfer enables strong electrostatic interactions between the Au^- and the CaO surface, boosted by a polaronic lattice distortion.[7,20] Thanks to this charge-mediated bond reinforcement triggered by the Mo, the gold tends to maximize its contact area with the CaO and forms 2D islands. A similar effect was earlier found for Au clusters on ultrathin oxide films,[12,13] only that the charging was initiated by electron tunneling from the metal substrate in that case. Also in the present example, the extra electrons most likely tunnel from the Mo dopants into the ad-metal, explaining why the 2D island shape prevails even in presence of a thin Mo-free capping layer.

In summary, the Mo-doping of CaO films changes the equilibrium shape of Au deposits from 3D to 2D. This crossover is initiated by a charge transfer from a high-lying Mo 4d level into the Au 6s affinity states, which makes the Au deposits negatively charged. The doping is highly efficient, as its signature remains detectable for Mo contents below 1 %. We suspect that similar effects are present in many industrial catalysts that always contain finite concentrations of impurity ions. In fact, some of the raft-shaped metal particles that are suggested to be particularly active in catalysis might result from an unintentional doping during catalyst preparation.[3]

Experimental Section

CaO films of 60 ML thickness were prepared by Ca deposition onto a sputtered and annealed Mo(001) single crystal in 5×10^{-7} mbar of oxygen. After annealing to 1000 K, an atomically flat and well-ordered oxide film is obtained, as deduced from a sharp (1×1) square pattern in LEED and STM images. The doping is realized by co-depositing small Mo amounts (2 %) from a second evaporator during oxide growth. The DFT calculations were performed with the projector-augmented plane-wave method (400 eV energy cutoff) as implemented in the VASP code.[21] PBE and hybrid HSE functionals with 25 % non-local exchange were used for calculating the total energies and the positions of Mo 4d levels inside the CaO band gap, respectively.[22,23] Whereas bulk CaO was modeled with a $(2\times2\times2)$ unit cell, a five-layer thick CaO(001) slab with a (3×3) surface cell and an Au atom adsorbed on one side was used for the adsorption studies. The Brillouin zone was sampled with a $(2\times2\times1)$ k-points mesh.

Received: July 29, 2011
Published online: October 11, 2011

[1] a) M. Haruta, T. Kobayashi, H. Sano, N. Yamada, *Chem. Lett.* **1987**, *16*, 405; b) M. Haruta, *CATTECH* **2002**, *6*, 102.
[2] M. Valden, X. Lai, D. W. Goodman, *Science* **1998**, *281*, 1647.
[3] a) A. S. K. Hashmi, G. J. Hutchings, *Angew. Chem.* **2006**, *118*, 8064; *Angew. Chem. Int. Ed.* **2006**, *45*, 7896; b) A. A. Herzing, C. J. Kiely, A. F. Albert, P. Landon, G. J. Hutchings, *Science* **2008**, *321*, 1331.
[4] T. Risse, S. Shaikhutdinov, N. Nilius, M. Sterrer, H.-J. Freund, *Acc. Chem. Res.* **2008**, *41*, 949.
[5] M. A. Brown, Y. Fujimori, F. Ringleb, X. Shao, F. Stavale, N. Nilius, M. Sterrer, H.-J. Freund, *J. Am. Chem. Soc.* **2011**, *133*, 10668.
[6] U. Landman, B. Yoon, C. Zhang, U. Heiz, M. Arenz, *Top. Catal.* **2007**, *44*, 145.
[7] G. Pacchioni, L. Giordano, M. Baistrocchi, *Phys. Rev. Lett.* **2005**, *94*, 226104.
[8] N. Nilius, M. V. Ganduglia-Pirovano, V. Brázdová, M. Kulawik, J. Sauer, H.-J. Freund, *Phys. Rev. Lett.* **2008**, *100*, 096802.
[9] G. Pacchioni, *J. Chem. Phys.* **2008**, *128*, 182505.
[10] V. Shapovalov, H. Metiu, *J. Catal.* **2007**, *245*, 205.
[11] N. Mammen, S. Narasimhan, S. de Gironcoli, *J. Am. Chem. Soc.* **2011**, *133*, 2801.
[12] D. Ricci, A. Bongiorno, G. Pacchioni, U. Landman, *Phys. Rev. Lett.* **2006**, *97*, 036106.
[13] M. Sterrer, T. Risse, M. Heyde, H.-P. Rust, H.-J. Freund, *Phys. Rev. Lett.* **2007**, *98*, 206103.
[14] a) H. Y. Kim, H. M. Lee, R. Ganesh, S. Pala, V. Shapovalov, H. Metiu, *J. Phys. Chem. C* **2008**, *112*, 12398; b) R. Ganesh, S. Pala, H. Metiu, *J. Phys. Chem. C* **2007**, *111*, 12715.
[15] X. Shao, P. Myrach, N. Nilius, H. J. Freund, *J. Phys. Chem. C* **2011**, *115*, 8784.
[16] a) M. Bäumer, H.-J. Freund, *Prog. Surf. Sci.* **1999**, *61*, 127; b) X. Lai, T. P. St Clair, M. Valden, D. W. Goodman, *Prog. Surf. Sci.* **1998**, *59*, 25.
[17] The high-spin configuration becomes favorable for Mo ions in the CaO surface.
[18] K. P. McKenna, A. L. Shluger, *Nat. Mater.* **2008**, *7*, 859.
[19] H. M. Benia, P. Myrach, A. Gonchar, T. Risse, N. Nilius, H.-J. Freund, *Phys. Rev. B* **2010**, *81*, 241415.
[20] U. Martinez, L. Giordano, G. Pacchioni, *ChemPhysChem* **2010**, *11*, 412.
[21] a) G. Kresse, J. Hafner, *Phys. Rev. B* **1993**, *47*, 558; b) G. Kresse, J. Furthmüller, *Phys. Rev. B* **1996**, *54*, 11169.
[22] J. Perdew, K. Burke, M. Ernzerhof, *Phys. Rev. Lett.* **1996**, *77*, 3865.
[23] a) J. Heyd, G. E. Scuseria, M. Ernzerhof, *J. Chem. Phys.* **2003**, *118*, 8207; b) J. Heyd, G. E. Scuseria, M. Ernzerhof, *J. Chem. Phys.* **2006**, *124*, 219906.